# Time-domain simulation of magnetic induction for modeling electrical conductivity anomalies in the Earth's mantle

Fumiko Tajima*

*Computational Science Division, Advanced Computing Center, RIKEN*

We carried out high performance computer simulations of electromagnetic (EM) responses induced by the coupling of external magnetic fields with the Earth's mantle using a newly developed time-domain 3-D finite difference code. Results show an observable difference of EM responses for different electrical conductivity distributions and that a high conductivity region in a narrow column (i.e., a plume like feature) can be detected.

## Introduction

Over the past decade seismology has made significant progress in using tomographic techniques for 3-D imaging of the elastic properties in the crust, mantle and core that dominates our present view of the Earth's interior. Although seismic waves provide good representations of elastic properties, they are not unambiguously sensitive to temperature, partial melt, or chemical compositions within the Earth.

In comparison, electrical conductivity is sensitive to such properties and can be measured by studying the frequency-dependent electromagnetic (EM) response in the Earth.[1,2] The lateral temperature contrast across a mantle convection cell is estimated to be in the range $10^2$ to $10^3$ K. For a dry crystalline mantle this contrast can map into approximately an order-of-magnitude lateral variation in conductivity,[3,4] and thus it presents a good prospect for 3-D image modeling. This order of magnitude of conductivity variation can be contrasted with the equivalent P- and S-wave velocity variation, which is in the range of within several percent.

The distribution of permanent observation sites of EM fields is extremely sparse,[5] which impeded efforts to construct detailed 3-D images of conductivity distribution in the mantle. On the other hand recent laboratory experiments provide conductivity data measured for various mantle minerals, and temperature ($T$) and pressure ($P$) conditions in the depth range from upper mantle transition zone to $\sim$1500 km.[6–9] Chemical composition and temperature in this depth range are fundamentally important for understanding mantle dynamics.

The present study aims to test if the EM responses for a suite of conductivity distributions have sufficient resolution and sensitivity for improving the mantle structural model developed by seismology.

* Permanent address: Seismological Laboratory, University of California Berkeley

## Anomalies associated with hot plumes

Recent 3-D global seismic tomography studies have captured stunning features of low velocity anomalies, which are almost continuous from the core mantle boundary into the upper mantle beneath Africa and the South Pacific.[10,11] The blurred image of low velocity anomaly with a lateral extent of over 2000 km may indicate a hot plume which is, however, assumed to be upwelling in a much narrower column. As mentioned above, seismic waves are not very sensitive to tempereture, partial melt, or chemical compositions that could distinguish hot plumes, and thus, the resolution of seismological approaches alone may be ultimately limited to constrain the structure of upwelling hot plumes.

On the other hand the electrical conductivity contrast due to the temperature anomaly in a hot plume can be as large as an order of magnitude. Here is an example of excercise to estimate the conductivity anomaly:

$$\sigma = \sigma_0 \exp\left(-\frac{\Delta H}{kT}\right), \tag{1}$$

where $\sigma_0$ is a preexponential factor, $T$ is temperature, $k$ is the Boltzmann constant, and the activation enthalpy $\Delta H = \Delta U + P\Delta V$ (where $\Delta U$ is activation energy, $\Delta V$ is activation volume, and $P$ is pressure).[7] Then the contrast of electrical conductivities across a mantle convection cell can be estimated as follows:

$$\ln\frac{\sigma'}{\sigma} = 11.605\Delta H\left(\frac{1}{T} - \frac{1}{T'}\right), \tag{2}$$

where $\sigma'$ is the conductivity in a hot plume. In the depth range of 410 to 660 km, $\Delta H \sim 1.29$ eV for wadsleyite and $\Delta H \sim 1.16$ eV for ringwoodite. The temperature contrast is $T' \sim 2300$ K vs $T \sim 1800$ K. Then, $\frac{\sigma'}{\sigma} \sim 5.7$. There are more measured conductivity values of mantle materials under the appropriate $P$ and $T$ conditions available from the recent laboratory experiments.[7–9]

## Sensitivity simulation of magnetic induction

A number of published papers presented results on the computer simulations of magnetic induction to model couplings with the mantle conductivity distribution, most of which, however, were carried out in the frequency domain. Recently Chou *et al.*[12,13] developed 3-D finite difference codes to solve the EM induction equations in the time domain both in Cartesian and spherical coordinates. These codes are designed to run on high performance computers with parallel processing. The time-domain codes have considerable advantages in dealing with transient EM fields such as magnetic substorms whose prominent frequency band is typically from ∼0.000005 to 0.00005 Hz. The codes have already been tested for performance speed and stability/convergence as well as the sensitivity of "skin depth" using simplified models of the mantle structure.[9,10] Here skin depth defines the sampling depth of EM waves as a function of frequency and conductivity.

We have carried out simulations of EM induction using the Cartesian code.[14] We tested EM responses for a variety of conductivity distributions using different conductivity values measured in the laboratory experiments. Figure 1 illustrates a hot plume, and examples of tested conductivity models with a variety of anomalies around the transition zone. An input plane electric field in the $x$-direction (or a vector potential $\mathbf{A}$ differentiated by time) that oscillates with a period of 50000 to 130000 sec (∼13 h to 2 days) represented the external field. We simulated EM responses to conductivity anomalies in a narrow vertical column of various sizes (with a diameter of 100 to 400 km) embedded in a depth range from 200 km to 1000 km with or without an overlying broader layer (∼$1000 \times 1000\,\mathrm{km}^2$) above the column. After sufficient computation time (3 to 5 times as long as the oscillation period of the external field), the induced magnetic field (IMF) at the surface was evaluated.

Results show an observable difference of EM responses for different conductivity distributions and that a high conductivity region in a narrow column can be detected.[14] The amplitude of the y-component IMF ($B_y$) above the anomalous conductivity distribution is as large as ∼120% of that induced without the anomaly (Fig. 2a). A magnetic field in the $z$-direction ($B_z$) is also induced by the anomalous 3-D

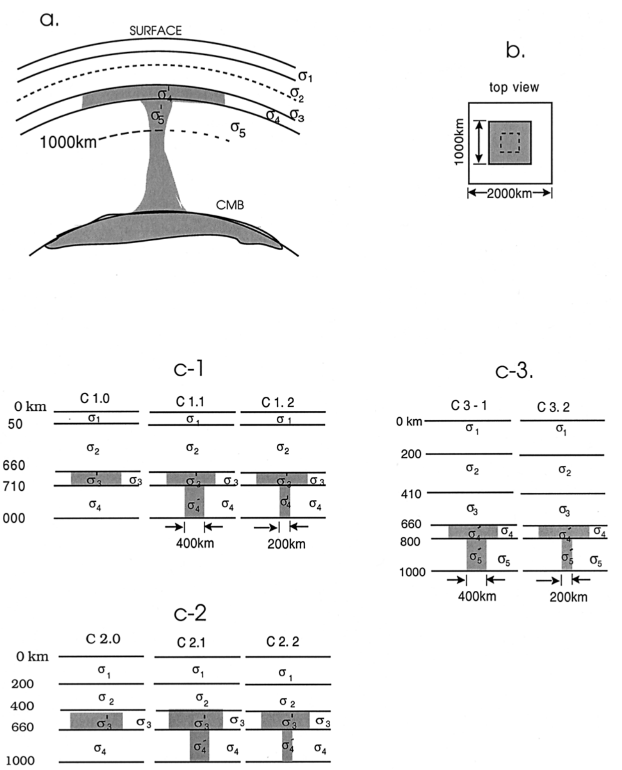


Fig. 1. (a) Illustration of a hot plume upwelling from the core-mantle boundary (CMB) in a layered structure of electrical conductivity. The shaded area is meant a hot plume in which the conductivity is higher. (b) Top view of the conductivity anomaly in the modeling with the Cartesian code. (c) Examples of models of conductivity anomalies for which the sensitivity of the magnetic induction has been tested using the Cartesian code.

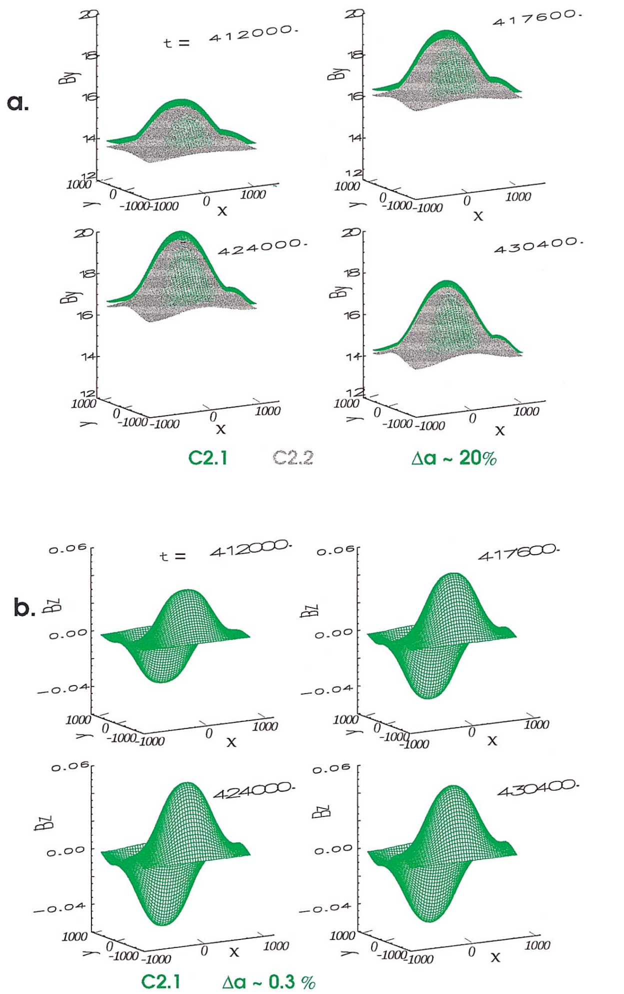


Fig. 2. (a) Induced magnetic fields in $y$-direction ($B_y$) associated with mantle conductivity anomalies at four different times (412000 s, 417600 s, 424000 s, and 430400 s) after the onset. (Models C2.1 shown in green and C2.2 in shade; see the illustration of the models in Fig. 1c). The input field is a plain sinusoidal electric field that oscillates in x-direction. The amplification of the $B_y$ above the conductivity anomaly is $\sim 20\%$ more than that outside the anomaly (see the illustrations for C2.1 and C2.2 in Fig1.c). (b) Corresponding magnetic fields induced in z-direction ($B_z$). The amplitudes are $\sim 0.3\%$ of the $B_y$). Note that without the 3-D anomaly the IMF should be a plain wave oscillating only in $y$-direction, and there will be no induction in $z$-direction.

conductivity distribution (Fig. 2b). Further, an IMF phase shift between locations away from the center of the anomaly can be observed.

## Discussion

The gap between the conjecture based on large-scale seismic tomographic images and the reality of mantle property measurements based on mineral physics is enormous. Combining electrical conductivity of deep-seated rocks with seismic models would provide a more powerful probe of mantle composition and state than would either property separately. The somewhat poorer resolving power of EM imaging techniques (diffusion equation) relative to seismic techniques (wave equation) is counterbalanced by the intense material property contrasts.[5] We thus continue carrying out computer simulations of EM induction by the coupling of external magnetic fields with mantle conductivity. Although we are using a simplified EM field imposed on the surface at present, the codes are flexible and have capability to incorporate observed data and expand to deal with naturally occurring powerful, low-frequency EM fields whose primary sources are located in the magnetosphere and ionosphere. Results from this simulational study will provide valuable assessments for integration of Earth models.

The author acknowledges the following scientists whose collaboration was essential for expanding this project: W. Chou and R. Matsumoto at Chiba University in code development, and T. Shankland at Los Alamos National Laboratory in providing with experimental results of electrical conductivity measurements. She also appreciates T. Ebisuzaki at RIKEN, who provided with access to the Fujitsu VPP700 computer.

## References

1) R. G. Roberts: Geophys. J. R. Astr. Soc. **85**, 583 (1986).
2) J. J. Roberts and J. A. Tyburczy: J. Geophys. Res. **104**, 7055 (1999).
3) T. J. Shankland, R. J. O'Connell, and H. S. Waff: Rev. Geophys. Space Phys. **19**, 394 (1981).
4) T. J. Shankland, J. Peyronneau, and J.-P. Poirier: Nature **366**, 453 (1993).
5) A. Schulz, R. D. Kurz, A. D. Chave, and A. G. Jones: Geophys. Res. Lett. **20**, 2941 (1993).
6) Y. Xu, C. McCammon, and B. T. Poe: Science **282**, 922 (1998).
7) Y. Xu, B. T. Poe, T. J. Shankland, and D. C. Rubie: Science **280**, 1415 (1998).
8) Y. Xu and T. J. Shankland: Geophys. Res. Lett. **26**, 2645 (1999).
9) Y. Xu, T. J. Shankland, and B. T. Poe: J. Geophys. Res. **105**, 27865 (2000).
10) J. Ritsema, H. J. van Hijist, and J. H. Woodhouse: Science **286**, 1925 (1999).
11) C. Mégnin and B. Romanowicz: Geophys. J. Int. **143**, 709 (2000).
12) W. Chou, R. Matsumoto, and F. Tajima: Comput. Phys. Commun. **131**, 26 (2000).
13) W. Chou, R. Matsumoto, and F. Tajima: Comput. Phys. Commun., 138/2, 175 (2001).
14) F. Tajima, T. Shankland, R. Matsumoto, and W. Chou: Earth, Planets Space (2001), to be submitted.